Interfacial-Dependent Morphologies in the Self-Organization System of Chiral Molecules Observed by Atomic Force Microscopy

ARTICLE *in* THE JOURNAL OF PHYSICAL CHEMISTRY B · FEBRUARY 2002

Impact Factor: 3.3 · DOI: 10.1021/jp0113681

7 AUTHORS, INCLUDING:

Yanjie Zhang
James Madison University
36 PUBLICATIONS **2,776** CITATIONS
SEE PROFILE

Ming Jin
Tongji University
95 PUBLICATIONS **1,906** CITATIONS
SEE PROFILE

Yanlin Song
Chinese Academy of Sciences
306 PUBLICATIONS **8,336** CITATIONS
SEE PROFILE

Interfacial-Dependent Morphologies in the Self-Organization System of Chiral Molecules Observed by Atomic Force Microscopy

Yan Jie Zhang,[†] Ming Jin,[†] Ran Lu,[†] Yanlin Song,[‡] Lei Jiang,*[,‡] Yingying Zhao,*[,†] and Tie Jin Li[†]

Department of Chemistry, Jilin University, Changchun, 130023, P. R. China, and Research Center for Molecular Sciences, Institute of Chemistry, Chinese Academy of Sciences, Beijing, 100080, P. R. China

Received: April 11, 2001; In Final Form: October 19, 2001

The interfacial-dependent self-organization of a chiral amino acid amphiphile is observed by atomic force microscopy (AFM). This chiral amino acid amphiphile possesses an amide group and two carboxyl groups that can form intermolecular hydrogen bonds in different forms, which corresponding to the two energy-minimum states exist in the aggregates of chiral molecules in one enantiomeric form. Three kinds of organizations were induced at different interfaces, which appear as helical aggregates on hydrophobic surface (e.g., highly oriented pyrolytic graphite (HOPG)), molecular flat layer, and superstructure layer on hydrophilic surface (e.g., mica). Moreover, these two energy-minimum states can also coexist in the same layer of the superstructure on an ordered hydrophobic surface made of the linearly aligned hydrocarbon chains. These phenomena experimentally prove the existence of double energy-minimum states in the chiral molecules that are in one enantiomeric form. The results presented here provide insight into how the interface can manipulate the bonding behavior in a multi-hydrogen bonding system and the self-organization of chiral molecules can be controlled consequently.

Introduction

Nanostructure science and technology has already played an important role in many scientific disciplines such as physics, chemistry, material science, biology, medicine, engineering, and computer simulation.[1−3] From the viewpoint of nanochemistry, molecular self-assembly and self-organization are increasingly significant for elucidation of life processes and the generation of new supramolecular structures or ensembles and molecular materials.[4] The design and synthesis of molecules that contain all the necessary information to organize themselves spontaneously into well-define nanostructures provide one of the most important challenges in supramolecular chemistry.[5,6] Much effort has been devoted to controlling the structures of the assemblies of synthetic molecules and macromolecules, opening the way for new applications.[7−17] Chirality is a very important phenomenon in nature. Crucial organic molecules associated with life (for example, amino acids, nucleic acids, and sugars) are chiral and usually occur in nature in only one of the two enantiomeric form.[18] To construct a stable interface composed of the supramolecular assembly of chiral molecules is significant.[19,20] It is generally agreed that the process of assembly of chiral molecules arises from one or more of several factors: the presence of chiral centers often induces helicity and decreases the crystallinity observed for racemates; directional attractive interactions such as hydrogen bonding or face-to-face $\pi-\pi$ aromatic stacking help generate linear arrays of molecules.[21,22]

In recent investigations we and others have found that the introduction of the competing interactions between two stable phases in the system could generate unusual interfacial phenomena and unique interfacial properties.[23,24] Here, we reported the interfacial-dependent self-organization of an amino acid amphiphile (*N*-stearyl-L-glutamic acid, C_{18}-Glu, Scheme 1) that possesses a chiral center and two carboxyl groups. Different forms of hydrogen bonding between molecules are presented, which may appear as two stable energy-minimum states in the aggregates. The cooperative competitive assembling process between them under peculiar conditions induced unusual interfacial structures. Three kinds of organizations were observed which appear as helical aggregates on HOPG, molecular flat layer, and superstructure layer on mica. The bonding behavior in this multi-hydrogen bonding system was controlled at different interfaces and the self-organization of chiral molecules was manipulated. C_{18}-Glu is somewhat similar to protein, having an acyl group neighboring an asymmetric carbon of amino acid

SCHEME 1: Chemical Structure of *N*-Stearoyl-L-glutamic Acid (C_{18}-Glu)

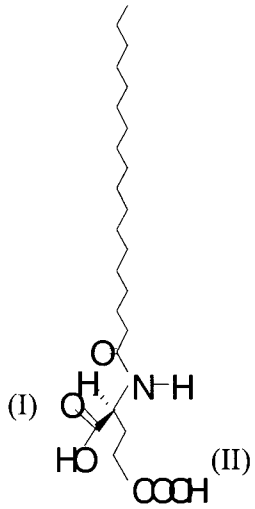

* Authors to whom correspondence should be addressed. Prof. Yingying Zhao, E-mail: zhyy@mail.jlu.edu.cn. Prof. Lei Jiang, E-mail: jianglei@infoc3.icas.ac.cn.

[†] Jilin University.

[‡] Research Center for Molecular Sciences, Institute of Chemistry, Chinese Academy of Sciences.

10.1021/jp0113681 CCC: $22.00
Published on Web 02/02/2002

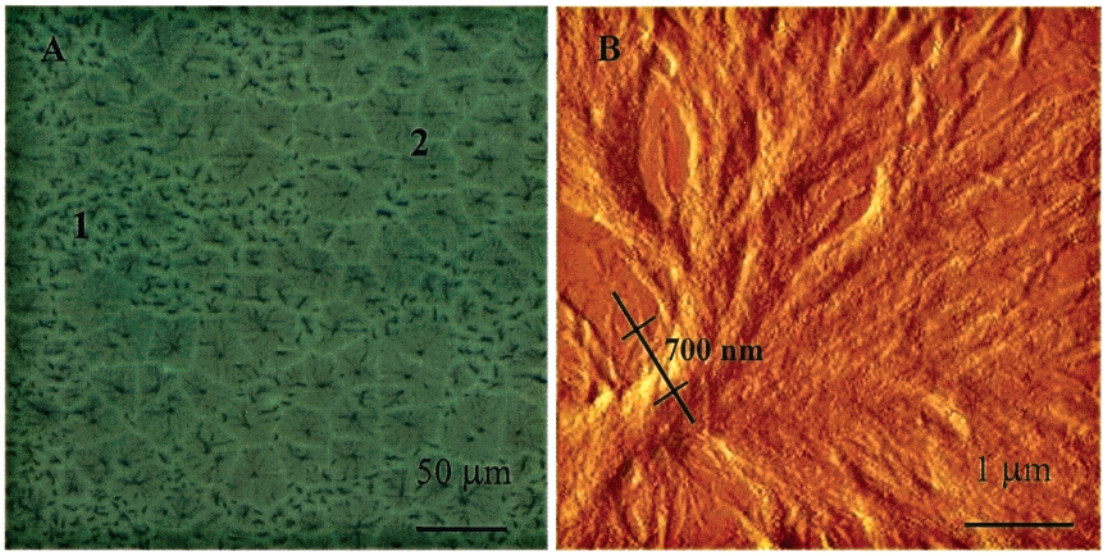

Figure 1. (A) A large-scale image (300 μm × 300 μm) of the fibrous assembly of C_{18}-Glu adsorbate on HOPG, obtained from the CCD camera of the scanning probe microscopy. (B) The AFM image of a helical aggregate adsorbate on HOPG (6 μm × 6 μm).

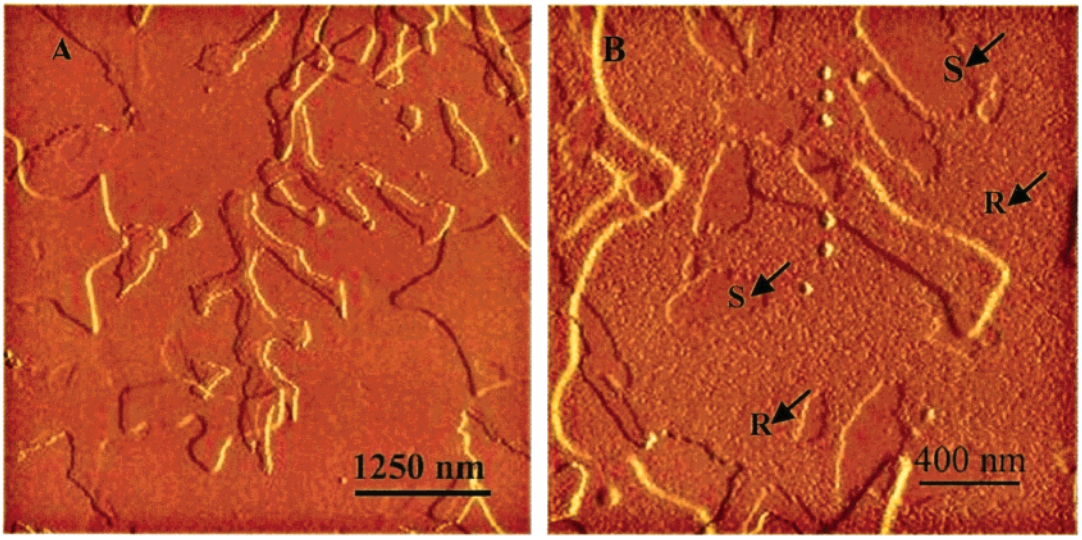

Figure 2. (A) AFM image of the flat-layered structure formed by C_{18}-Glu adsorbate on the mica surface (5 μm × 5 μm). (B) A zoomed-in image of (A) (2 μm × 2 μm), the roughness over the surface is not uniform, smooth areas and rough areas are labled as **S** and **R**, respectively.

and being sufficiently amphiphilic to interact with both hydrophobic and hydrophilic surroundings. Thus, an investigation of the chiral aggregates of C_{18}-Glu would be of interest as regards the structure and function of proteins. The control over the self-organization of C_{18}-Glu may provide a useful method to change the structure of proteins.

Experimental Section

N-Stearyl-L-glutamic acid (C_{18}-Glu, Scheme 1) was synthesized from stearyl chloride and L-glutamic acid by the method described by M. Takehara et al.[25] C_{18}-Glu was dissolved in ethanol to form a solution with the concentration of 1×10^{-2} M. A drop of C_{18}-Glu solution was applied to the substrates, and studied by AFM after solvent had evaporated slowly. Substrates were freshly cleaved planes of HOPG and mica (10 mm × 10 mm). The AFM investigations were carried out using a commercial system (Seiko Instruments Inc., SPA300HV, Japan) with a 20 μm scanner. A triangular-shaped Si_3N_4 cantilever with spring constant of 0.02 N m^{-1} was used to acquire images in contact mode. The image gathered from CCD camera was obtained on SPA3800 instrument (Seiko Instruments Inc.). All images were recorded under ambient conditions at 22 °C. The scan directions in all images were maintained uniform. Each of the images presented here was the representation of several images taken at different times to ensure reproducibility.

Results and Discussion

A large-scale image (300 μm × 300 μm) gathered by a CCD camera on the scanning probe microscopy obtained on the dried C_{18}-Glu adsorbate on HOPG is shown in Figure 1A. Many aggregates in mesoscale were observed. The size of aggregates can be divided into two categories: < 10 μm × 10 μm, and about 20−40 μm × 20−40 μm, which are indicated as **1** and **2** in Figure 1A. This is similar to the other chiral amphiphiles that formed helical twisted fibers.[26−33] The aggregates can be observed more clearly in the AFM image (Figure 1B, 6 μm × 6 μm). Each bundle of the aggregates is a left-twisted helix

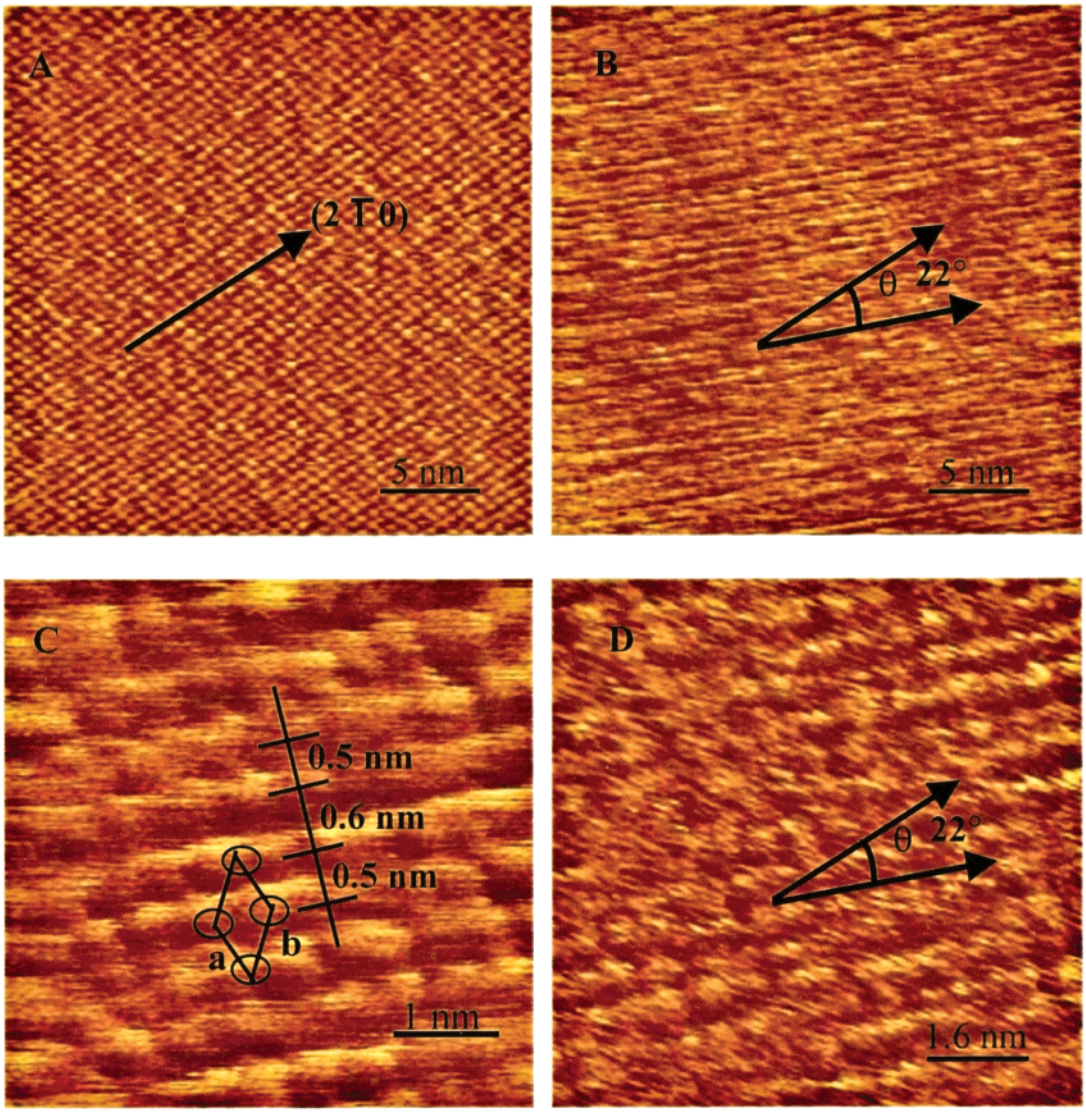

Figure 3. (A) AFM image of the mica surface at the atomic scale in the air. (B) High-resolution AFM image obtained from the smooth area, the angle $\theta = 22°$ is the angle between the (2 $\bar{1}$ 0) direction of (0001) face of mica and the direction of molecular alignment. (C) Zoomed-in image of (B), *a* and *b* indicated the molecular crystal lattice. (D) High-resolution image obtained from the rough area (corresponding to the hydrophilic area), the direction of the hydrophilic lines is the same as that in (B).

and contains many left-handedly twisted fibers tangled up together. While on mica surface, the chiral molecules assembled to a molecular flat-layered structure in a very long-range order (Figure 2A). Several layers with irregular boundary are presented. Detailed observation shows that the roughness of the top surface on mica is not uniform (Figure 2B), i.e., some areas are smooth and some areas are rough indicated as **S** and **R,** respectively. The smooth areas are corresponding to hydrophobic surfaces and the rough areas correspond to the hydrophilic surfaces, which will be discussed in detail.

Figure 3A is the AFM image of mica surface at the atomic scale in the air. The molecular resolution images obtained from smooth areas and rough areas are shown in Figure 3B and Figure 3D, respectively. The molecules closely packed linearly and the lines are parallel to each other. It also shows some preferential orientation over the surface. From the zoomed-in image (Figure 3C) one can observed the crystal lattice clearly. The height cross section taken in the direction perpendicular to the lines shows that the most of molecules packed in a regular sawtooth pattern with a period of two molecules. The distance between two molecules in the same period is about 0.5 nm and that of the adjacent period is about 0.6 nm (shown in Figure 3C). A few molecules are not packed in this pattern and commensurate the defect of the structure.[34] The lines in Figure 3D correspond to the close packing of the headgroups (carboxyl groups) of C_{18}-Glu and the direction of the lines is the same as that in Figure 3B. That is, the headgroups and the hydrocarbon chains are packed in the same direction between different layers. These results indicated that the molecules in the upper layer (exposed the hydrophilic surface) are aligned along the lines formed by hydrocarbon chains in the next layer below them. There is an angle $\theta = 22°$ between the (2 $\bar{1}$ 0) direction of (0001) face of mica and the lines formed in both hydrophobic and hydrophilic areas indicated in Figure 3B and 3D. These results demonstrate a template effect of mica to the self-organization process.

These two kinds of morphologies on HOPG and mica may come from the different molecular orientations of this chiral amphiphile. According to Nandi's effective pair potential (EPP) approach,[35,36] the EPP for chiral molecules depends on the size

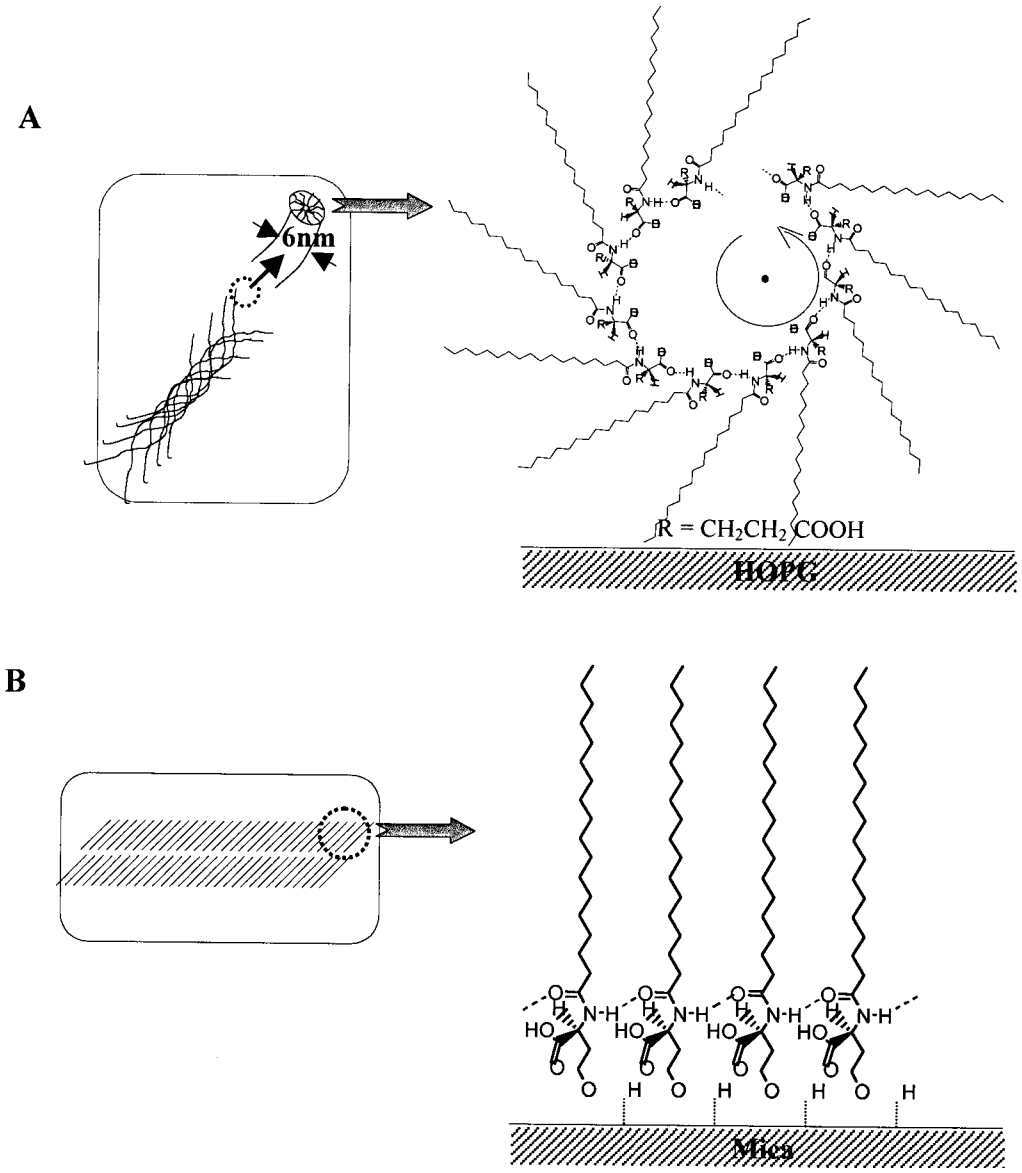

Figure 4. (A) Schematic representation of hydrogen bonding network of the single helical fiber of C_{18}-Glu in ethanol solution, many single fibers tangled up together to form the helical aggregates. (B) Schematic representation of the hydrogen bonding network in the layered structure on the mica surface.

of the groups attached to the chiral center, their separation distance, and their relative orientation. The minimal energy conformation of a d−d or l−l pair shows double energy-minimum states, with one minimum at a twist angle between adjacent two molecules and at a short distance (Twist State), while the second, at nearly zero degree but at large separation (Linear State). For the present molecule, it can be involved in three stable intermolecular hydrogen bondings. The first one is between −NH− and −CO− in carboxyl group attached to the chiral center of the molecule that results in Twist State. The second one is between −NH− and −CO− in amide group that induces a stable Linear State. The third one is between carboxyl groups separated by two $-CH_2-$ groups from the chiral center. The changes in hydrogen bonding forms at different interfaces will induce various morphologies.

In the alcoholic solution, Twist State is effective forming helical aggregates and there are free carboxyl groups in the aggregates.[37] Figure 4A illustrates the hydrogen bonding in the single helical fiber formed in ethanol solution. The hydrocarbon chains exposed to the solution. If we take the estimation of the dimension of the molecule as about 3.1 nm calculated from the energy-minimum configuration of C_{18}-Glu, the diameter of the single helical fiber would be about 6 nm. Many single helical fibers tangled up together to form the helical aggregates in ethanol solution. When a drop of solution was applied to the hydrophobic surface of HOPG, the exposed hydrophobic hydrocarbon chains of the helical aggregates in ethanol solution will attach to the surface. The two ends of each bundle of the helical aggregates will cover the HOPG surface to the furthest extent and the fan-shape structure at each end is formed. Similarly, helically twisted fibers from glucosamide bolaamphiphiles had been also observed by transmission electron microscopic (TEM).[33] However, on a hydrophilic surface of mica, the free carboxyl group of C_{18}-Glu in the helical aggregates sticks to the surface via hydrogen bonding and the hydrophobic hydrocarbon chains extend upward. The hydrogen bonding in the helical aggregates is broken and lateral hydrogen bonding network between adjacent amide groups appears (Figure 4B). The helical aggregates assemble to a flat-layered structure showing Linear State. The interactions between the molecules in the first layer and the mica surface play a key role in the self-organization process. Figure 5 illustrates the assembling process from a drop

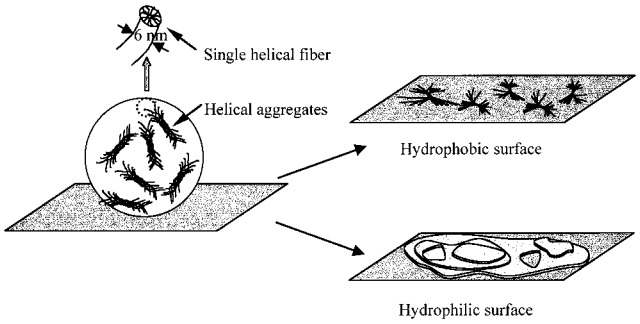

Figure 5. The illustration of the assembling process of a drop of solution to helical aggregates on a hydrophobic surface and flat-layered structure on a hydrophilic surface.

of solution to the helical aggregates on hydrophobic surface and flat-layered structure on a hydrophilic surface.

To investigate these interesting phenomena, the layered structure on mica surface was studied in detail. The topographic image and the friction force mapping of edges of different layers were obtained simultaneously (Figure 6A and 6B). The friction force mapping is based on the frictional interactions between the chemical functional groups at the outermost few angstroms of microscopic contacting area.[38] The topographic image shows that the film is composed of four regions, each with different height (Figure 6A). The friction force mapping showed a clear correspondence with the domains in the topographic image. Brightness in the friction force mapping corresponds to a high value of surface free energies.[39] These results indicate that the layered structure is composed of the alternation of hydrophobic surface and hydrophilic surface. The smooth area corresponds to the hydrophobic alkyl chains and the rough surface corresponds to the hydrophilic carboxyl groups. Cross-sectional analysis along the lines marked AB (Figure 6C) and CD (Figure 6D) in Figure 6A shows two steps with the height of about 0.9 $\pm$ 0.05 nm and 3.1 $\pm$ 0.1 nm. The layer with the height of 3.1 $\pm$ 0.1 nm corresponds to the full extension of molecules C_{18}-Glu. 0.9 nm $\pm$ 0.05 nm corresponds to the difference between the inclined double layer and the fully extended monolayer, and the details will be discussed as follows.

Figure 7A and the zoomed-in image (Figure 7B) are obtained from the rough areas. It was found that the molecular arrangement is not in a complete disorder but in parallel stripes, i.e., superstructure. Similar superstructure formed on the C_{60} single crystal was also reported in the literature.[40,41] That superstructure derived from the coexistence of two stable phases, i.e., face-centered cubic and hexagonal-close-packed phases. The anisotropic growth of the self-organization system is indicated by the arrows. The mean peak-to-peak spacing is about 12−18 nm and 8−10 nm in the directions shown as a_1 and b_1, respectively. The corrugation height differences (ΔH) of the rough surface are about 0.3 $\pm$ 0.05 nm. The directions a_1 and b_1 are identical to the crystal lattice of the molecules in the high-resolution

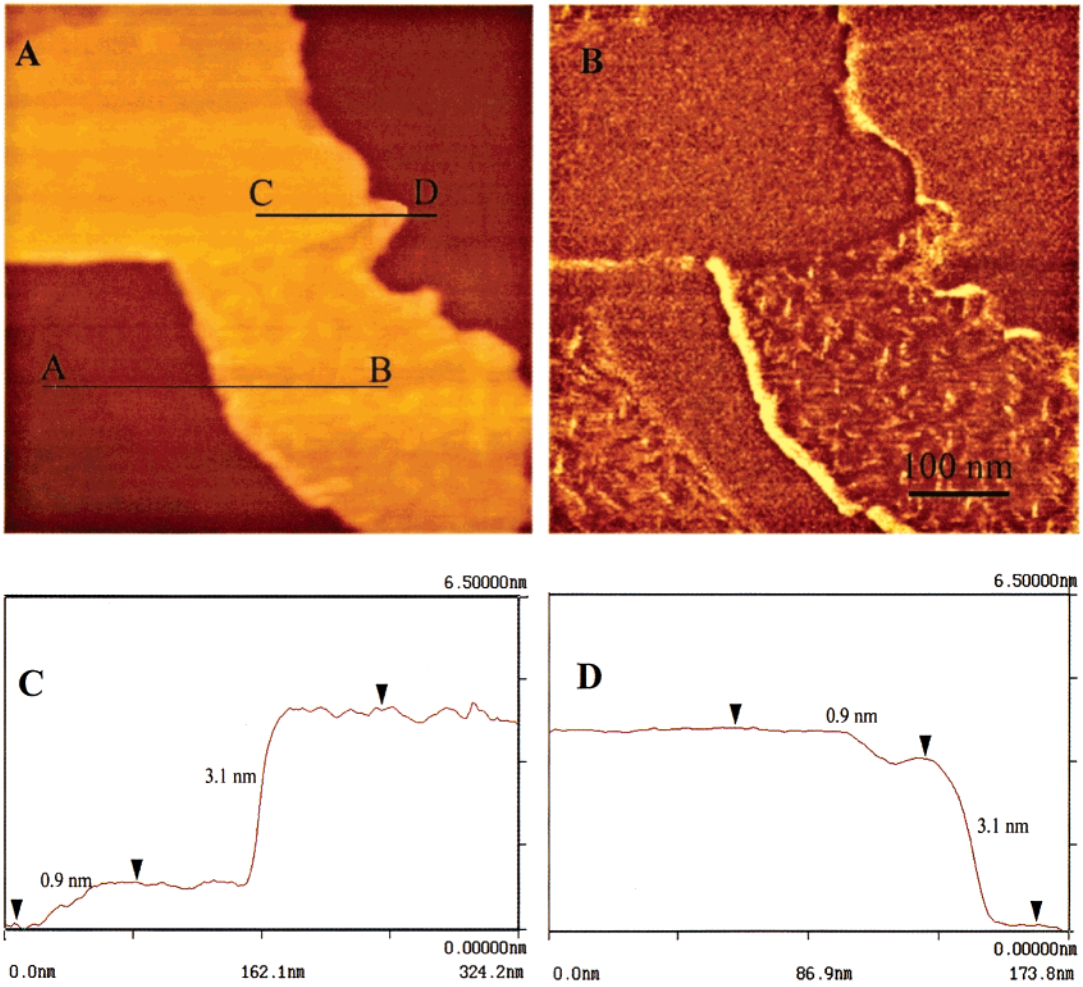

Figure 6. (A) 500 nm × 500 nm topographic image of C_{18}-Glu on a mica surface. (B) The friction force mapping of (A), high brightness in this image corresponds to a high value of surface free energy, (A) and (B) were recorded simultaneously. (C) Cross-sectional analysis along the line drawn in the direction of AB. (D) Cross-sectional analysis along the line drawn in the direction of CD.

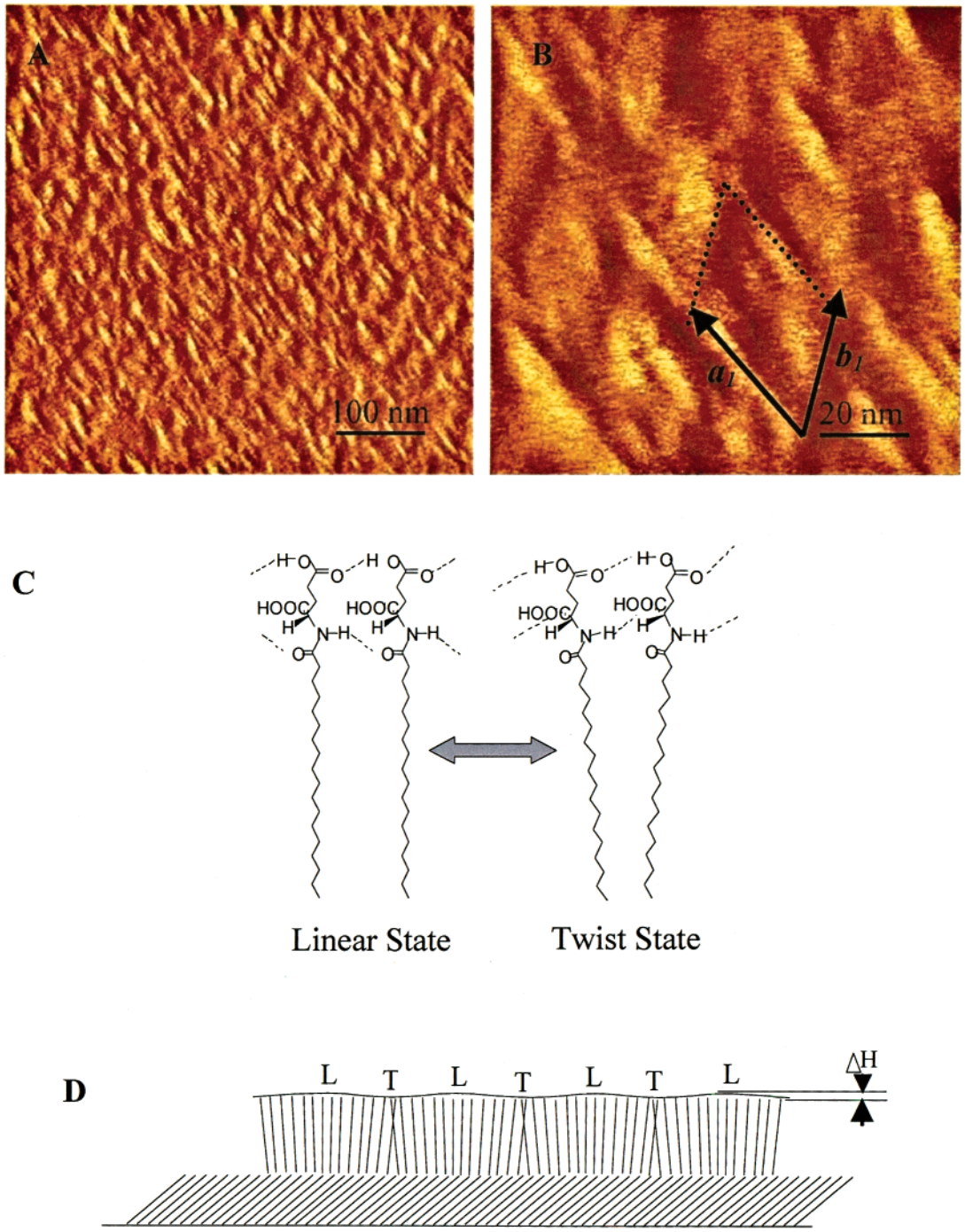

Figure 7. (A) AFM image taken from the rough area. (B) A zoomed-in image of (A), a_1, b_1, and arrows show the orientation of anisotropic growth. (C) The molecular packing in the superstructure, a pair of C_{18}-Glu molecules favors little twists from neighbor to neighbor in a transition state from Linear State to Twist State. (D) Illustration of the formation of superstructure.

image (Figure 3C) shown as *a* and *b*. Since the molecular distance is about 0.6 nm, there will be about 20−30 molecules in a period along the a_1 direction and 13−16 molecules along the b_1 direction. The corrugation over the surface in this system come from the partial dislocation corresponding to the transition from Linear States to Twist States stacking.

To clarify the layered structure, a diluted solution was applied to the mica surface. Figure 8A is the layered structure adsorbed on mica surface. Cross-sectional analysis (8B) along the line marked *ab* shows a step with the height of about 2.0 ± 0.1 nm, which corresponding to a monolayer. Molecules incline to an angle θ about 50° ($\cos\theta = 2.0/3.1$) relative to the normal of the surface in the first layer. As shown in Scheme 1, two carboxyl groups in the molecule C_{18}-Glu are at different steric position. One of them (carboxyl I) is attached to the chiral center directly and another (carboxyl II) is linked by two $-CH_2-$ groups to the chiral center. Carboxyl II can move more freely than carboxyl I and can adjust the location of the molecule to match the crystal lattice of mica well. Since amide functional groups possess the Z configuration structure for long-chain molecules,[42] chiral molecules assemble regularly and match with each other to form an intermolecular hydrogen bonding network. In the first layer, all the molecules packed in Linear State to develop the structure that schematically are shown in Figure 4B. After the first layer had grown on the mica surface, the surface became hydrophobic with the

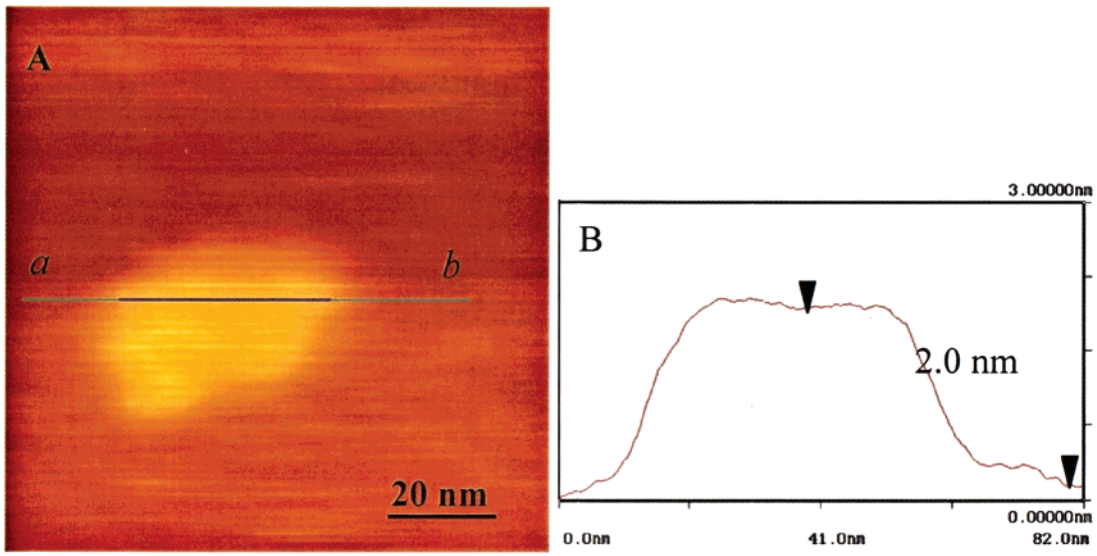

Figure 8. (A) AFM image of the monolayer adsorbate on a mica surface, which was obtained from a diluted solution (2×10^{-3} M). (B) Cross-sectional analysis along the line drawn in the direction of *ab* shown in (A).

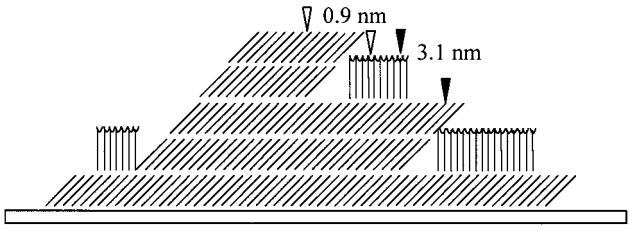

Figure 9. Structural model of the layered structure formed by C_{18}-Glu on mica, viewed at the cross section.

lines composed of hydrocarbon chains aligned parallel to each other.

As for the self-organization in the second layer, the molecules aligned along the hydrophobic lines formed by the first layer, but two stable orientations were observed within the same layer. For the first one, molecules almost perpendicular to the substrate surface and carboxyl II formed hydrogen bonds between each other that are indicated in Figure 7C. Once this assembly had been formed, there were no chances to form the interlayer hydrogen bonds to grow the next layer. The hydrophilic headgroups exposed to the air and the superstructure formed. Meanwhile, the molecules in this layer interact with other molecules by a cooperative interlayer hydrogen bond forming inclined double layers. In this area, molecules packed in the Linear State to give symmetric assembling. On the third layer it can grow the layered structure repetitively like that on the first layer. Figure 9 is a structural model of this assembly constructed according to the analysis above.

The most interesting thing is that on the rough surface it manifests a twist tendency in the linear alignment. In this area, the driving force to form the condensed packing in a superstructure is the competition between Twist State and Linear State at an ordered hydrophobic interface. This interface composed of highly ordered hydrocarbon chains. At this interface, carboxyl groups linked to $-CH_2-$ were set free from hydrogen bonding with the substrate, but formed intermolecular hydrogen bonding between each other that is indicated in Figure 7C. While −NH− can be involved in intermolecular hydrogen bonding in two extreme forms. One is between −NH− and −CO− in the amide group that induces molecular packing labeled as the Linear State. The other is between −NH− and −CO− in carboxyl group attached to the chiral center of the molecule that induces the Twist State. These two stacking forms may coexist in the same layer through a stacking transition from the Linear State site to the Twist State site or vice versa. A pair of the chiral molecules favors a little twist between them and there is a change of the molecular orientation from neighbor to neighbor. The hydrogen bonding network in this layer is not in the same plane completely, but in a little curvature. On the other hand, the template effect of the hydrophobic surface of the layer has a tendency to induce the Linear State. Molecules in this layer aligned along the hydrophobic line composed of the hydrocarbon chains in the next layer below. Under usual conditions, the configuration in a little twist leads to a curvature for the free-standing molecules at the air−water interface.[43,44] But in this area, the microscopic curvature cannot develop to a macroscopic structure. The molecules packed in a certain period and stopped due to the template effect of the ordered hydrophobic surface then restarted a new cycle. The superstructure formed with the hydrophilic headgroups exposed to the air. Figure 7D illustrated the formation of the superstructure. This phenomenon proved the coexistence of the double energy-minimum states for the pairwise chiral molecules in the same enantiomeric form[35,36] at microscopic scale. The competition between them induced a special superstructure, which the macroscopic rough surface (Figure 7A) manifested the twist tendency and the molecular image (Figure 3D) suggested the linear alignment in microscopic scale.

The hydrogen bonding networks formed in the aggregates on HOPG and mica are somewhat similar to the α-helix and β-sheet in protein. Thus the study of the aggregates of C_{18}-Glu would be of significance to investigate the structure and the function of proteins. One can suppose that if a proper interface is provided, the α-helix may be changed to a β-sheet and the structure and function of protein would change accordingly.

Conclusion

The interfacial-dependent self-organization of a kind of chiral amino acid amphiphile (C_{18}-Glu) was investigated by AFM. It formed helical aggregates on the hydrophobic surface and molecular flat-layered structure and superstructure on the hydrophilic surface. The competition between the double energy-minimum states for chiral amphiphiles has been demonstrated

both in mesoscopic and microscopic scales. The results presented here provide insight into how the interface can manipulate the bonding behavior in a multi-hydrogen bonding system and the self-organization of chiral molecules can be controlled consequently. Such control over the surface morphology may be valuable in designing a new interface that is an entity of the irregular structure in macroscale and the highly ordered array in nanoscale. This kind of knowledge should be very useful in biological recognition and specificity. This also maybe provides a useful method to control the structure of proteins.

Acknowledgment. The authors acknowledge the National Natural Science Foundation of China (NNSFC), State Key Project Fundamental Research and Chinese Academy of Sciences for financial support.

References and Notes

(1) *Nanotechnology Research Directions: IWGN Workshop Report, Vision for Nanotechnology R&D in the Next Decade*; Roco, M. C., Williams, R. S., Alivisatos, P., Eds.; International Technology Research Institute, World Technology (WTEC) Division, 1999.

(2) Siegel, R. W.; Hu, E.; Cox, D. M.; Goronkin, H.; Jelinski, L.; Mendel, J.; Roco, M. C.; Shaw, D. T. *WTEC Panel Report on Nanostructure Science and Technology, R&D Status and Trends in Nanoparticles, Nanostructured Materials, and Nanodevices*, WTEC Hyper-Librarian, 1999.

(3) Stupp, S. I.; LeBonheur, V.; Walker, K.; Li, L. S.; Huggins, K. E.; Keser, M.; Amstutz, A. *Science* **1997**, *276*, 384.

(4) Auzély-Velty, R.; Benvegnu, T.; Plusquellec, D.; Mackenzie, G.; Haley, J. A.; Goodby, J. W. *Angew. Chem., Int. Ed. Engl.* **1998**, *37*, 2511.

(5) Jolliffe, K A.; Timmerman, P.; Reinhoudt, D. N. *Angew. Chem., Int. Ed.* **1999**, *38*, 933.

(6) Lehn, J.-M. *Supramolecular Chemistry, Concept and Perspectives*; VCH: Weinhein, 1995.

(7) Yamaguchi, N.; Nagvekar, D. S.; Gibson, H. W. *Angew. Chem., Int. Ed.* **1998**, *37*, 2361.

(8) Jenekhe, S. A.; Chen, X. L. *Science* **1999**, *283*, 372.

(9) Jenekhe, S. A.; Chen, X. L. *Science* **1998**, *279*, 1903.

(10) Yang, W.; Chai, X.; Chi, L.; Liu, X.; Cao, Y.; Lu, R.; Jiang, Y.; Tang, X.; Fuchs, H.; Li, T. J. *Chem. Eur. J.* **1999**, *5*, 1144.

(11) Yam, C. M.; Kakkar, A. K. *Langmuir* **1999**, *15*, 3807.

(12) Owens, R. W.; Smith, D. A. *Langmuir* **2000**, *16*, 562.

(13) Vollmer, M. S.; Clark, T. D.; Steinem, C.; Ghadiri, M. R. *Angew. Chem., Int. Ed. Engl.* **1999**, *38*, 1598.

(14) Sijbesma, R. P.; Beijer, F. H.; Brunsveld, L.; Folmer, B. J. B.; Hirschberg, J. H. K. K.; Lange, R. F. M.; Lowe, J. K. L.; Meijer, E. W. *Science* **1997**, *278*, 1601.

(15) Rivera, J. M.; Martín, T.; Rebek, J., Jr. *Science* **1999**, *279*, 1021.

(16) Engelkamp, H.; Middelbeek, S.; Nolte, R. J. M. *Science* **1999**, *284*, 785.

(17) Harada, A.; Kataoka, K. *Science* **1999**, *283*, 65.

(18) Auer, F.; Schubert, D. W.; Stamm, M.; Arnebrant, T.; Swietlow, A.; Zizlsperger, M.; Sellergren, B. *Chem. Eur. J.* **1999**, *5*, 1150.

(19) Lorenzo, M. O.; Baddeley, C. J.; Muryn, C.; Raval, R. *Nature* **2000**, *404*, 376.

(20) Lorenzo, M. O.; Haq, S.; Bertrams, T.; Murray, P.; Raval, R.; Baddeley, C. J. *J. Phys. Chem. B* **1999**, *103*, 10661.

(21) Oda, R.; Huc, I.; Candau, S. J. *Angew. Chem., Int. Ed. Engl.* **1998**, *37*, 2689.

(22) Oda, R.; Huc, I.; Schmutz, M.; Candau, S. J.; Mackintosh, F. C. *Nature* **1999**, *399*, 566.

(23) Seul, M.; Andelman, D. *Science* **1995**, *267*, 476.

(24) Jiang, L.; Wang, R.; Yang, B.; Li, T. J.; Tryk, D. A.; Fujishima, A.; Hashimoto, K.; Zhu, D. B. *Pure Appl. Chem.* **2000**, *12*, 73, and references therein.

(25) Takehara, M.; Yoshimura, I.; Takizawa, K.; Yoshida, R. *J. Am. Oil. Chem. Soc.* **1972**, *49*, 157.

(26) Fuhrhop, J.-H.; Helfrich, W. *Chem. Rev.* **1993**, *93*, 1565.

(27) Nakashima, N.; Asakuma, S.; Kunitake, T. *J. Am. Chem. Soc.* **1985**, *107*, 509.

(28) Fuhrhop, J.-H.; Schnieder, P.; Boekema, E.; Helfrich, W. *J. Am. Chem. Soc.* **1988**, *110*, 2861.

(29) Fuhrhop, J.-H.; Boettcher, C. *J. Am. Chem. Soc.* **1990**, *112*, 1768.

(30) Shimizu, T.; Masuda, M. *J. Am. Chem. Soc.* **1997**, *119*, 2812.

(31) Masuda, M.; Hanada, T.; Yase, K.; Shimizu, T. *Macromolecules* **1998**, *31*, 9403.

(32) Kogiso, M.; Ohnishi, S.; Yase, K.; Masuda, M.; Shimizu, T. *Langmuir* **1998**, *14*, 4978.

(33) Nakazawa, I.; Masuda, M.; Okada, Y.; Hanada, T.; Yase, K.; Asai, M.; Shimizu, T. *Langmuir* **1999**, *15*, 4757.

(34) Schwartz, D. K.; Viswanathan, R.; Zasadzinski, J. A. N. *Langmuir* **1993**, *9*, 1384.

(35) Nandi, N.; Bagchi, B. *J. Am. Chem. Soc.* **1996**, *118*, 11208.

(36) Nandi, N.; Bagchi, B. *J. Phys. Chem. A* **1997**, *101*, 1343.

(37) Sakamoto, K.; Hatano, M. *Bull. Chem. Soc. Jpn.* **1980**, *53*, 339.

(38) Green, J.-B. D.; McDermott, M. T.; Porter, M. D.; Siperko, L. M. *J. Phys. Chem.* **1995**, *99*, 10960.

(39) Takano, H.; Kenseth, J. R.; Wong, S.-S.; O'Brien, J. C.; Porter, M. D. *Chem. Rev.* **1999**, *99*, 2845.

(40) Jiang, L.; Kim, Y.; Iyoda, T.; Li, J.; Kitazawa, K.; Fujishima, A.; Hashimoto, K. *Adv. Mater.* **1999**, *11*, 649.

(41) Jiang, L.; Iyoda, T.; Tryk, D. A.; Li, J.; Kitazawa, K.; Fujishima, A.; Hashimoto, K. *J. Phys. Chem. B* **1998**, *102*, 6351.

(42) Du, X.; Shi, B.; Liang, Y. *Langmuir* **1998**, *14*, 3631.

(43) Vollhardt, D.; Emrich, G.; Gutberlet, T.; Fuhrhop, J.-H. *Langmuir* **1996**, *12*, 5659, and references therein.

(44) Parazak, P.; Uang, J. Y.-J.; Turner, B.; Stine, K. J. *Langmuir* **1994**, *10*, 3787. and references therein.